

RESEARCH ARTICLE

View Article Online
View Journal | View IssueCite this: *Inorg. Chem. Front.*, 2024,
11, 6190Remarkable enhancement of Ca²⁺ affinity using a redox-switchable coordinating group†Juan Pedro Merino, ^{a,b} Adrián M. Abelairas, ^a Javier Hernández-Ferrer, ^c
Ana M. Benito, ^c Wolfgang K. Maser, ^c José L. Vilas-Vilela, ^{b,d}
David Esteban-Gómez, ^a Alejandro Criado, ^a Jesús Mosquera ^{*a} and
Carlos Platas-Iglesias ^{*a}

Redox-switchable coordinating groups hold significant promise for metal purification, detection, and the design of stimuli-responsive materials. However, existing designs often involve complex structures where a redox-active metal interferes with the target metal interaction. In this study, we demonstrate the use of a simple organic motif, namely 2-nitropyridine, as a redox-switchable coordinating group. This group was conjugated with a diaza-crown ether to yield a ligand for Ca²⁺ coordination. Under normal conditions, this ligand demonstrates weak metal interactions attributed to the electronic properties of the nitro groups. However, upon reduction, it transitions to a radical anion state with a strong affinity for Ca²⁺. Notably, the required redox potential shifts depending on the metal ion present in the solution, dictated by the charge density of the complexed ion. This behavior facilitates the recognition of various metal ions in a solution, opening possibilities for applications in biological or industrial sensing.

Received 16th July 2024,
Accepted 1st August 2024

DOI: 10.1039/d4qi01612b

rsc.li/frontiers-inorganic

Introduction

Responsive materials are poised at the forefront of scientific research and technological innovation,¹ offering the potential to revolutionize domains like medicine, electronics, and energy storage.^{2–4} These versatile materials exhibit adaptability in response to external stimuli like pH, light, or redox potential. Notably, redox-responsive materials are particularly significant in industry for their capability to employ electrons as a versatile trigger, offering promising applications across various domains.⁵

A specific category of redox-responsive materials encompasses those equipped with redox-switchable coordinating groups.⁶ These groups exhibit a remarkable ability to selectively bind or release metals in direct response to changes in electrical potential. To date, the structural diversity of redox-

switchable coordinating groups is quite limited. Most examples are grounded in metal complexes, where the oxidation state of the metallic center significantly influences the donor capacity of adjacent atoms for the target metal.^{6–11} A variation of this strategy has been recently published where an *ortho*-substituted *closo*-carborane was applied for the reversible capture of uranyl ions.¹² Other notable examples include redox-responsive groups capable of releasing metals, such as Ca²⁺, upon oxidation.^{13–15}

Building upon the pioneered work by Kaifer *et al.*, where nitrobenzyl groups were employed as redox-switchable entities to enhance the affinity of crown ethers for sodium,¹⁶ herein we explore the application of 2-nitropyridine as a redox-switchable coordinating group for recognizing Ca²⁺. The Ca²⁺ ion plays a key role in several physiological processes including the signaling pathways of the nervous system.¹⁷ Electrochemical sensors represent the most promising alternative to overcome several limitations of luminescence sensors, to allow real-time monitoring of Ca²⁺ in live brains.^{18,19}

In its native state, the nitro moiety manifests limited coordinating capacity, accompanied by its electron-withdrawing characteristics, which concurrently diminish the Lewis basicity of the pyridine. However, upon reduction, the nitro moiety might undergo a transformative process, evolving into its radical anion form. This transition would endow 2-nitropyridine with the attributes of a robust bidentate coordinating group, facilitating effective metal binding. Significantly, thanks to its chemical simplicity and remarkable stability, this

^aCentro Interdisciplinar de Química e Bioloxía (CICA) and Departamento de Química, Facultade de Ciencias, Universidade da Coruña, 15071 A Coruña, Spain.
E-mail: carlos.platas.iglesias@udc.es

^bMacromolecular Chemistry Research Group (labquimac), Department of Physical Chemistry, Faculty of Science and Technology, University of the Basque Country (UPV/EHU), 48940 Leioa, Spain

^cInstituto de Carboquímica (ICB-CSIC), C/Miguel Luesma Castán 4, 50018 Zaragoza, Spain

^dBC Materials, Basque Center for Materials, Applications and Nanostructures, UPV/EHU Science Park, 48940 Leioa, Spain

† Electronic supplementary information (ESI) available. See DOI: <https://doi.org/10.1039/d4qi01612b>



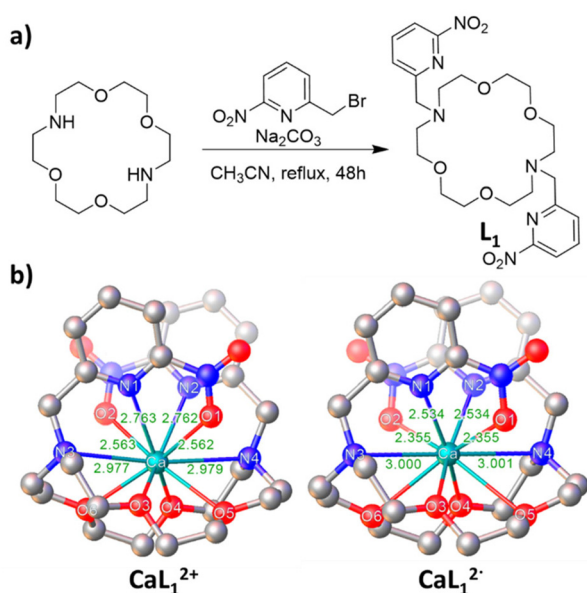


Fig. 1 (a) Synthesis of L_1 . (b) DFT models illustrating the complexation of L_1 to Ca^{2+} in its oxidized form, CaL_1^{2+} , and upon the formation of the radical anion in both nitro-pyridine, *i.e.*, $CaL_1^{2\bullet-}$.

group can be effortlessly incorporated into the targeted chemical framework, offering a direct pathway for the development of novel redox-switchable ligands.

To check our hypothesis, we decided to couple 2-nitropyridine to a diaza-crown ether (Fig. 1). Crown ethers are extensively applied as building blocks in the field of supramolecular chemistry due to their unique capabilities to recognize metal cations.²⁰ They have a distinct cavity size and charge distribution that allows for selective recognition of a metal cation with a specific dimension. This ligand was inspired in MACROPA, a well-known chelator containing pyridinecarboxylate groups, which was developed for selective complexation of large metal ions.^{21–24}

Results and discussion

Design, synthesis and electrochemical characterization of receptor L_1

A primary advantage of 2-nitropyridine is its chemical simplicity. Numerous commercially available analogs of this molecule simplify their direct incorporation into the desired platform. Specifically, L_1 was prepared in quantitative yield by treating 4,13-diaza-18-crown-6 with 2-(bromomethyl)-6-nitropyridine in acetonitrile in the presence of sodium carbonate as base (reflux, 48 h, Fig. 1a). We envisaged that the poor coordinating ability of the pendant arms will result in weak binding to alkaline and alkaline-earth cations, while electrochemical reduction will result in strong coordination of the pendant arms after formation of the radical anion form. DFT studies supported this design, as the CaL_1^{2+} complex is characterized by a weak coordination of the 2-nitropyridine units, with Ca–N

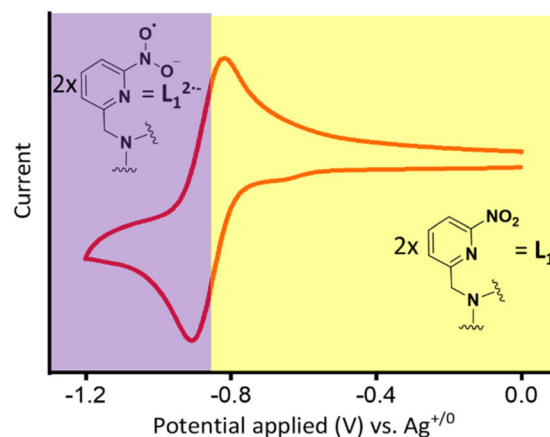


Fig. 2 Cyclic voltammogram for L_1 (1 mM) in acetonitrile with 0.1 M of NBu_4PF_6 as supporting electrolyte. The signal was recorded with a glassy carbon electrode (scan rate of 500 mV s^{-1}).

and Ca–O distances of 2.763 and 2.563 Å, respectively. These distances decrease dramatically upon reduction of the system, amounting to 2.543 (Ca–N) and 2.385 Å (Ca–O) in $CaL_1^{2\bullet-}$ (Fig. 1b, see ESI† for computational details).

The cyclic voltammogram (CV) of an acetonitrile solution of L_1 (0.1 M NBu_4PF_6) shows a single electrochemically *quasi*-reversible reduction occurring at a $E_{1/2}$ value of -864 mV versus the silver couple (Ag^+/Ag^0 , Fig. 2). According to literature, the reduction of the nitro group attached to aromatic compounds is strongly influenced by the nature of the solvent.²⁵ In aprotic solvents, nitrobenzene can undergo up to two consecutive one-electron reduction steps, yielding the radical anion and the dianion successively (Scheme S1†).²⁶ Both steps are reversible, however the dianion tends to react rapidly with solvent, electrolytes or impurities. Analyzing (eqn (S1)†) the CV of L_1 with the Randles–Sevcik equation, gives an electron number of $1.6 e^-$ for the standard equation, and $1.9 e^-$ for the equation with parameters corrected by Matsuda.²⁷ This is consistent with the expected behavior of nitro groups in acetonitrile,²⁸ and thus a two-electron reaction can be unequivocally assumed, with each nitropyridine group contributing one electron. With this insight, we can infer that the observed *quasi*-reversible process is attributed to the formation of a dianion with one electron on each nitrobenzene. Additionally, the presence of a singular redox couple suggests that both active redox groups are sufficiently separated in space, ensuring that the reduction of the first group, yielding $L_1^{\bullet-}$, does not influence the subsequent reduction leading to the formation of $L_1^{2\bullet-}$.

Electrochemical response of L_1 in the presence of Ca^{2+} and affinity constants

The CV of L_1 was replicated following the addition of 1 equiv. of calcium trifluoromethanesulfonate [$Ca(OTf)_2$]. Strikingly, the resulting CV profile significantly deviates from that of L_1 in the absence of metal (Fig. 3a). The primary distinction arises from the observation of two *quasi*-reversible redox



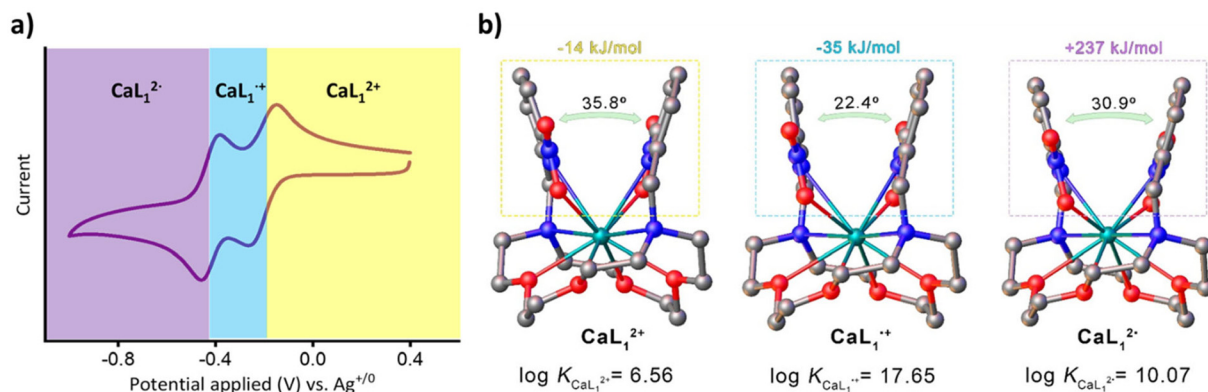


Fig. 3 (a) Cyclic voltammogram of an acetonitrile solution of L_1 (1 mM) in the presence of one equivalent of calcium trifluoromethanesulfonate. NBu_4PF_6 (0.1 M) was used as supporting electrolyte and the signal was recorded with a glassy carbon electrode (scan rate of 500 mV s^{-1}). (b) DFT simulations of the three complexes observed on the cyclic voltammogram, showcasing the angles between the nitropyridines in each scenario. The DFT interaction energy between the nitropyridines within each structure in gas phase is displayed atop. At the bottom, the experimental affinity constants for Ca^{2+} with each oxidation state of L_1 are provided.

couples rather than one. We propose that, unlike the scenario in the absence of the metal, the interaction with the Ca^{2+} ion forces the two nitropyridine groups into proximity, leading to repulsion between the radical anions and hindering the second reduction.

The second notable distinction pertains to the $E_{1/2}$ values, which exhibit a noteworthy anodic shift potential. Specifically, the $E_{1/2}$ value for the initial reduction is -208 mV , and for the subsequent reduction, it is -416 mV . Thus, the initial reduction shifted by 0.656 V respect to L_1 in the absence of metal. This substantial variance is associated with the distinct affinity constants of L_1^{2-} , L_1^- , and L_1^{\cdot} for Ca^{2+} . Thus, a UV-vis absorption spectrophotometric titration was applied to determine the affinity constant of L_1 for Ca^{2+} in the conditions applied in the CV experiments, specifically $0.1\text{ M } NBu_4PF_6$ in acetonitrile at room temperature. The absorption spectrum of L_1 experiences significant changes upon addition of Ca^{2+} , with the absorption maximum at 278 nm undergoing a blue shift to 274 nm , with well-defined isosbestic points developing during the titration (Fig. S9, ESI†). The spectrophotometric data were successfully fitted to a 1:1 binding isotherm with a binding constant of $K = 3.6(1) \times 10^6\text{ M}^{-1}$ using standard methods (see ESI† for details).²⁹ This value, along with the variation in reduction potentials observed in the presence of calcium, was utilized to derive the affinity constants of the reduced ligands with eqn (1):

$$E_{CaL} - E_L = \frac{RT}{F} \ln \frac{K_{CaL^-}}{K_{CaL}} \quad (1)$$

An analogous expression was employed to estimate the association constant of L_1^{2-} (see ESI† for details). Previous studies used an analogous expression to estimate the stability of complexes when the metal ion is the redox-active species.^{30,31}

L_1^{\cdot} showed the highest affinity constant for Ca^{2+} , attaining an extraordinary $\log K$ value of 17.65 . The Ca^{2+} complexes with

the highest stabilities are formed with anionic ligands such as $DOTA^{4-}$, reaching a $\log K$ value of 17.2 .³² To our knowledge, this signifies the highest reported affinity constant for this cation. For comparison, complexes with crown ethers and cryptates are characterized by $\log K$ values <7.0 , although some Ca^{2+} cryptates were found to be particularly inert.³³ The structurally related $MACROPA^{2-}$ forms a Ca^{2+} complex with $\log K$ value of 5.25 in aqueous medium.³⁴ Regarding other redox-switchable hemilabile ligands, information on their affinities is frequently unreported. However, it is anticipated that the reduced form of these ligands would demonstrate a significantly lower affinity for this ion, attributed to their dependence on redox-active metals. In contrast to L_1 , where the reduction induces the formation of strong coordinating groups, the reduction in other ligands occurs over a metal that is not directly coordinated with Ca^{2+} , leading to a reduction in electrostatic interaction.

Interestingly, the fully reduced form of L_1 , denoted as L_1^{2-} , displays a lower affinity compared to the aforementioned intermediate, with a $\log K$ value of 10.07 . The unexpected lower affinity of L_1^{2-} could be ascribed, at least in part, to the repulsion that arises between the two radical anions when they are in proximity and interacting with the metal. Indeed, the angle defined by the least square planes of the aromatic units in the DFT structure of CaL_1^{2+} (35.8°) decreases to 22.4° in $CaL_1^{+\cdot}$, suggesting attractive interactions among the two aromatic units in the latter. This interaction energy between the two arms was estimated by DFT to be $\sim -35\text{ kJ mol}^{-1}$ in $CaL_1^{+\cdot}$. However, DFT predicts a very important repulsive interaction between the pendant arms in CaL_1^{2-} ($+237\text{ kJ mol}^{-1}$, Fig. 3b). DFT provides $\Delta G_{(sol)}^\circ$ values for the first and second reduction processes of -286 and -259 kJ mol^{-1} , in line with the CV data that shows that the first reduction is more favorable than the second. The energy difference among the two processes corresponds to a difference in potential of $\Delta E = 270\text{ mV}$, in reasonable agreement with the experimental data of 208 mV . The



analysis of kinetic electrochemical parameters (Table S1†) also agrees with a process involving significant changes in conformational and solvation energies.³⁵

The former findings suggest that a modified version of the L_1 ligand, featuring a single redox-switchable coordinating group, is anticipated to display a solitary *quasi*-reversible redox couple upon coordination with Ca^{2+} , aligning closely with the initial reduction potential of L_1 . To test this hypothesis, we synthesized ligand L_2 , differing from L_1 by the absence of one of the 2-nitropyridine moieties. As expected, L_2 exhibited a single redox couple for both the molecule in the absence and presence of Ca^{2+} with $E_{1/2}$ values of -811 and -225 mV respectively (Fig. 4).

Electrochemical response of L_1 in the presence of different cations

To get further insights on the performance of L_1 as redox-switchable ligand, we recorded CV experiments in the presence of equimolar quantities of additional redox-inactive mono- and di-positive metal ions, namely, Na^+ , K^+ , Ca^{2+} , Sr^{2+} and Ba^{2+} . All the cations exhibited a behavior akin to Ca^{2+} , with two distinct redox couples observed at potentials more positive than those recorded for the ligand in its original state (Fig. 5). As depicted in Fig. 5, among the Group 2 cations, Sr^{2+} exhibited $E_{1/2}$ values that closely resembled those of Ca^{2+} at -284 and -451 mV, followed by Ba^{2+} , with values of -341 and -494 mV. In contrast, alkali metals displayed values much more similar to the original ligand, with Na^+ at -580 and -811 mV and K^+ , at -757 and -888 mV. On this basis, it can be concluded that, (i) in all cases, $L_1^{•-}$, has a larger affinity for

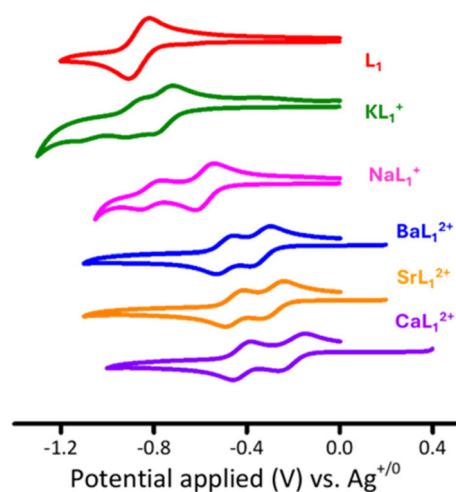


Fig. 5 Cyclic voltammogram of an acetonitrile solution of L_1 (1 mM) with different alkaline and alkaline earth metals. NBu_4PF_6 (0.1 M) was used as supporting electrolyte and the signal was recorded with a glassy carbon electrode (scan rate of 500 $mV s^{-1}$).

the metals than the fully reduced L_1^{2-} , and (ii) the impact of reduction on the affinity for the metals follows the order $Ca^{2+} > Sr^{2+}, Ba^{2+} \gg Na^+ > K^+$. Akin to previously reported redox-switchable coordinating groups, this order correlates with the Lewis acidity of the cations, directly linked to the charge density of the metal ions. It has been shown that the Lewis acidity of metal ions correlates very well with the pK_a of the aquated ions,³⁶ which have been demonstrated to be very good descriptors of Lewis acidity.³⁷ Indeed, the plots of the observed $E_{1/2}$ values versus the pK_a data of the corresponding aqua-ions are linear, with the potential becoming more negative as the pK_a increases (Fig. S8, ESI†). The quality of the linear regression is particularly good for the first reduction wave ($R^2 > 0.995$). The poorer linear correlation of the second reduction wave ($R^2 > 0.95$) suggests that the repulsive effects among the two reduced nitropyridine groups depend significantly on the size of the metal ion.

Conclusions

In conclusion, our findings show that 2-nitropyridine effectively functions as a redox-switchable coordinating group. Its limited coordinating capabilities change dramatically upon reduction, forming a robust bidentate ligand. Leveraging its chemical simplicity, we integrated this group into a diaza-crown ether framework, yielding a redox-responsive ligand finely tuned for the biorelevant Ca^{2+} cation. This ligand allows attaining unprecedented affinity for Ca^{2+} upon its reduction (log K value of 17.65). The principles presented here will allow the design of electrochemical sensors for Ca^{2+} and other metal ions, which requires anchoring the electroactive ligand on the surface of electrodes.

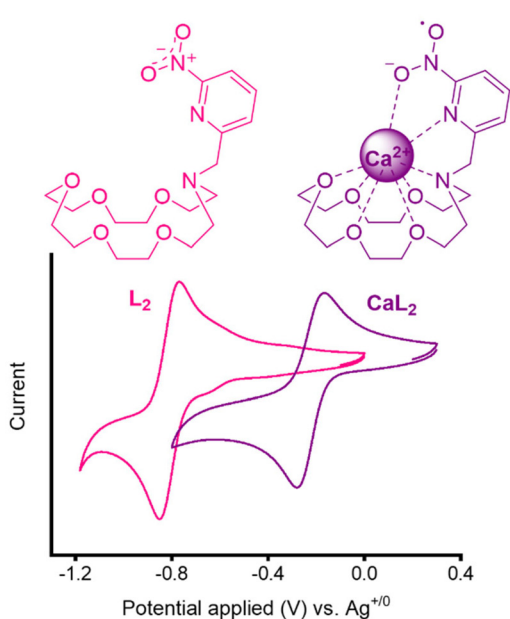


Fig. 4 Cyclic voltammogram of an acetonitrile solution of L_2 (1 mM) in the absence and in the presence of one equivalent of Ca^{2+} . NBu_4PF_6 (0.1 M) was used as supporting electrolyte and the signal was recorded with a glassy carbon electrode (scan rate of 500 $mV s^{-1}$).



Data availability

The data supporting this article have been included as part of the ESI.†

Conflicts of interest

There are no conflicts to declare.

Acknowledgements

The authors acknowledge financial support from MCIN/AEI/10.13039/501100011033 and “ESF Investing in your future”: RYC2020-030183-I and PID2021-127002NA-I00 (A. C.) RYC2019-027842-I (J. M.), PID2022-138335NB-I00 (C. P.-I.). Financial support from Xunta de Galicia (ED431C 2023/33 and ED431F 2022/02), Gobierno de Aragón (DGA, T03_23R), and Government of the Basque Country (Grupos de Investigación IT1756-22) are also acknowledged. J. P. M. acknowledges a Margarita Salas postdoctoral grant under the “Convocatoria de ayudas para la recualificación del sistema universitario español para 2012–2023”.

References

- X. Xia, C. M. Spadaccini and J. R. Greer, Responsive materials architected in space and time, *Nat. Rev. Mater.*, 2022, **7**, 683–701.
- S. Khizar, N. Zine, A. Errachid and A. Elaissari, in *Stimuli-Responsive Materials for Biomedical Applications*, American Chemical Society, 2023, vol. 1436, pp. 1–30.
- Z. Wei, L. Yu, S. Lu and Y. Zhao, Reversibly thermo-responsive materials applied in lithium batteries, *Energy Storage Mater.*, 2023, **61**, 102901.
- S.-H. Byun, J. Y. Sim, K.-C. Agno and J.-W. Jeong, Materials and manufacturing strategies for mechanically transformative electronics, *Mater. Today Adv.*, 2020, **7**, 100089.
- T. Fukino, H. Yamagishi and T. Aida, Redox-Responsive Molecular Systems and Materials, *Adv. Mater.*, 2017, **29**, 1603888.
- H. F. Cheng, A. I. d’Aquino, J. Barroso-Flores and C. A. Mirkin, A Redox-Switchable, Allosteric Coordination Complex, *J. Am. Chem. Soc.*, 2018, **140**, 14590–14594.
- A. M. Allgeier and C. A. Mirkin, Ligand Design for Electrochemically Controlling Stoichiometric and Catalytic Reactivity of Transition Metals, *Angew. Chem., Int. Ed.*, 1998, **37**, 894–908.
- A. H. Reath, J. W. Ziller, C. Tsay, A. J. Ryan and J. Y. Yang, Redox Potential and Electronic Structure Effects of Proximal Nonredox Active Cations in Cobalt Schiff Base Complexes, *Inorg. Chem.*, 2017, **56**, 3713–3718.
- C. M. Dopp, R. R. Golwankar, S. R. Kelsey, J. T. Douglas, A. N. Erickson, A. G. Oliver, C. S. Day, V. W. Day and J. D. Blakemore, Vanadyl as a Spectroscopic Probe of Tunable Ligand Donor Strength in Bimetallic Complexes, *Inorg. Chem.*, 2023, **62**, 9827–9843.
- E. Y. Tsui, R. Tran, J. Yano and T. Agapie, Redox-inactive metals modulate the reduction potential in heterometallic manganese–oxido clusters, *Nat. Chem.*, 2013, **5**, 293–299.
- T. K. Ghosh, S. Maity, S. Ghosh, R. M. Gomila, A. Frontera and A. Ghosh, Role of Redox-Inactive Metal Ions in Modulating the Reduction Potential of Uranyl Schiff Base Complexes: Detailed Experimental and Theoretical Studies, *Inorg. Chem.*, 2022, **61**, 7130–7142.
- M. Keener, C. Hunt, T. G. Carroll, V. Kampel, R. Dobrovetsky, T. W. Hayton and G. Ménard, Redox-switchable carboranes for uranium capture and release, *Nature*, 2020, **577**, 652–655.
- C. Amatore, D. Genovese, E. Maisonhaute, N. Raouafi and B. Schöllhorn, Electrochemically Driven Release of Picomole Amounts of Calcium Ions with Temporal and Spatial Resolution, *Angew. Chem., Int. Ed.*, 2008, **47**, 5211–5214.
- K. X. Bhattacharyya, L. Boubekur-Lecaque, I. Tapsoba, E. Maisonhaute, B. Schöllhorn and C. Amatore, An organometallic derivative of a BAPTA ligand: towards electrochemically controlled cation release in biocompatible media, *Chem. Commun.*, 2011, **47**, 5199–5201.
- K. X. Bhattacharyya, L. Boubekur-Lecaque, I. Tapsoba, E. Maisonhaute, B. Schöllhorn and C. Amatore, Water-soluble, redox-active organometallic calcium chelators, *Dalton Trans.*, 2012, **41**, 14257–14264.
- A. Kaifer, L. Echegoyen, D. A. Gustowski, D. M. Goli and G. W. Gokel, Enhanced sodium cation binding by electrochemically reduced nitrobenzene-substituted lariat ethers, *J. Am. Chem. Soc.*, 1983, **105**, 7168–7169.
- A. M. Hofer and E. M. Brown, Extracellular calcium sensing and signalling, *Nat. Rev. Mol. Cell Biol.*, 2003, **4**, 530–538.
- Y. Liu, Z. Liu, Y. Zhou and Y. Tian, Implantable Electrochemical Sensors for Brain Research, *JACS Au*, 2023, **3**, 1572–1582.
- F. Zhao, Y. Liu, H. Dong, S. Feng, G. Shi, L. Lin and Y. Tian, An Electrochemophysiological Microarray for Real-Time Monitoring and Quantification of Multiple Ions in the Brain of a Freely Moving Rat, *Angew. Chem., Int. Ed.*, 2020, **59**, 10426–10430.
- G. W. Gokel, W. M. Leevy and M. E. Weber, Crown Ethers: Sensors for Ions and Molecular Scaffolds for Materials and Biological Models, *Chem. Rev.*, 2004, **104**, 2723–2750.
- N. A. Thiele, S. N. MacMillan and J. J. Wilson, Rapid Dissolution of BaSO₄ by Macropa, an 18-Membered Macrocyclic Receptor with High Affinity for Ba²⁺, *J. Am. Chem. Soc.*, 2018, **140**, 17071–17078.
- R. Ferreirós-Martínez, D. Esteban-Gómez, É. Tóth, A. de Blas, C. Platas-Iglesias and T. Rodríguez-Blas, Macrocyclic Receptor Showing Extremely High Sr(II)/Ca(II) and Pb(II)/Ca(II) Selectivities with Potential Application in Chelation Treatment of Metal Intoxication, *Inorg. Chem.*, 2011, **50**, 3772–3784.



- 23 A. Roca-Sabio, M. Mato-Iglesias, D. Esteban-Gómez, É. Tóth, A. de Blas, C. Platas-Iglesias and T. Rodríguez-Blas, Macrocyclic Receptor Exhibiting Unprecedented Selectivity for Light Lanthanides, *J. Am. Chem. Soc.*, 2009, **131**, 3331–3341.
- 24 N. A. Thiele, V. Brown, J. M. Kelly, A. Amor-Coarasa, U. Jermilova, S. N. MacMillan, A. Nikolopoulou, S. Ponnala, C. F. Ramogida, A. K. H. Robertson, C. Rodríguez-Rodríguez, P. Schaffer, C. Williams, J. W. Babich, V. Radchenko and J. J. Wilson, An Eighteen-Membered Macrocyclic Ligand for Actinium-225 Targeted Alpha Therapy, *Angew. Chem., Int. Ed.*, 2017, **56**, 14712–14717.
- 25 J. H. Wagenknecht, Reaction of electrogenerated nitrobenzene radical anion with alkyl halides, *J. Org. Chem.*, 1977, **42**, 1836–1838.
- 26 A. Kuhn, K. G. von Eschwege and J. Conradie, Reduction potentials of para-substituted nitrobenzenes—an infrared, nuclear magnetic resonance, and density functional theory study, *J. Phys. Org. Chem.*, 2012, **25**, 58–68.
- 27 H. Matsuda and Y. Ayabe, Zur Theorie der Randles-Sevčikschen Kathodenstrahl-Polarographie, *Z. Elektrochem.*, 1955, **59**, 494–503.
- 28 T. Wirtanen, E. Rodrigo and S. R. Waldvogel, Recent Advances in the Electrochemical Reduction of Substrates Involving N–O Bonds, *Adv. Synth. Catal.*, 2020, **362**, 2088–2101.
- 29 P. Gans, A. Sabatini and A. Vacca, Investigation of equilibria in solution. Determination of equilibrium constants with the HYPERQUAD suite of programs, *Talanta*, 1996, **43**, 1739–1753.
- 30 M. Regueiro-Figueroa, J. L. Barriada, A. Pallier, D. Esteban-Gómez, A. de Blas, T. Rodríguez-Blas, É. Tóth and C. Platas-Iglesias, Stabilizing Divalent Europium in Aqueous Solution Using Size-Discrimination and Electrostatic Effects, *Inorg. Chem.*, 2015, **54**, 4940–4952.
- 31 L. Burai, É. Tóth, G. Moreau, A. Sour, R. Scopelliti and A. E. Merbach, Novel Macrocyclic EuII Complexes: Fast Water Exchange Related to an Extreme M–Owater Distance, *Chem. – Eur. J.*, 2003, **9**, 1394–1404.
- 32 G. Anderegg, F. Arnaud-Neu, R. Delgado, J. Felcman and K. Popov, Critical evaluation of stability constants of metal complexes of complexones for biomedical and environmental applications* (IUPAC Technical Report), *Pure Appl. Chem.*, 2005, **77**, 1445–1495.
- 33 M. F. K. Trautnitz, T. Haas, H. Schubert and M. Seitz, Unexpected discovery of calcium cryptates with exceptional stability, *Chem. Commun.*, 2020, **56**, 9874–9877.
- 34 R. Ferreirós-Martínez, D. Esteban-Gómez, É. Tóth, A. de Blas, C. Platas-Iglesias and T. Rodríguez-Blas, Macrocyclic Receptor Showing Extremely High Sr(II)/Ca(II) and Pb(II)/Ca(II) Selectivities with Potential Application in Chelation Treatment of Metal Intoxication, *Inorg. Chem.*, 2011, **50**, 3772–3784.
- 35 B. Fabre, J.-P. Desvergne, M. Colomès and J. Simonet, Electrochemical oxidation in different media of bis(*p*-phenylene crown ether) as a symmetrical molecule bearing two identical redox centers, *J. Electroanal. Chem.*, 1999, **460**, 119–134.
- 36 D. D. Perrin, in *Ionisation Constants of Inorganic Acids and Bases in Aqueous Solution (Second Edition)*, ed. D. D. Perrin, Pergamon, 2nd edn, 1982, pp. 1–138.
- 37 A. Kumar and J. D. Blakemore, On the Use of Aqueous Metal-Aqua pKa Values as a Descriptor of Lewis Acidity, *Inorg. Chem.*, 2021, **60**, 1107–1115.

